

# Anodization of n and p-GaAs in ethylene glycol–water–tartaric acid mixture

Ma. BUDA, D. CENGER, D. DIACONESCU

*Institute of Physics and Technology of Materials, PO Box MG7, Magurele, Bucharest, Romania*

M. BUDA\*

*“POLITEHNICA” University of Bucharest, Department of Applied Physical Chemistry and Electrochemistry, Calea Grivitei 132, 78122, Bucharest, Romania*

Received 29 November 1996; revised 9 June 1997

This paper describes the pulsed constant current anodization of n<sup>+</sup> and p<sup>+</sup>-GaAs in ethylene glycol–water–tartaric acid (AGW) mixture, up to 17 mA cm<sup>-2</sup>. A 0.26 μm thick film is obtained for a final voltage of 135 V at 4.3 mA cm<sup>-2</sup> pulsed current density. Cyclic voltammetry showed that the initial growth of a monolayer anodic oxide can be described by a charge transfer with uncompensated cell resistance model. The relationship between peak current, peak voltage and scan rate has been verified for this process, based on the above model.

Keywords: *GaAs, pulsed current anodization, cyclic voltammetry, chronopotentiometry, anodic oxides*

## 1. Introduction

The growth of anodic layers on GaAs in different media has been studied since the early 1970s. Anodic oxides can be used to define laser diode stripes and to achieve very well controlled etch for precise ridge waveguide configurations. Hasegawa and Hartnagel [1], found that acid–glycol–water (AGW) mixtures ensure stable and reproducible anodic films on GaAs. The anodic oxidations were performed in d.c. conditions (constant voltage or current density). The constant current density technique is preferred because it provides constant growth rate. Recently, results on anodic oxides obtained in pulsed voltage conditions showed that the anodic layers grow more uniformly [2, 3]. This paper describes a study of anodic oxides in AGW mixtures, using pulsed current conditions for lower current densities (up to 17 mA cm<sup>-2</sup>).

## 2. Experimental details

### 2.1. Pulsed constant current anodization of GaAs

Anodic oxidation of GaAs under constant current density conditions was performed using a home-made pulsed constant current source. Highly doped GaAs substrates (2 × 10<sup>18</sup> cm<sup>-3</sup>) were used for anodization at room temperature (20 °C) in AGW solution (2% tartaric acid aqueous solution with pH 6 in a 1 : 2 mixture with ethylene glycol). Fischer and Teare recommended [4] a constant continuous current density value of 1 mA cm<sup>-2</sup>. In our study we used

current density values from 1.24 to 17 mA cm<sup>-2</sup>. Higher current densities allow faster growth of the anodic oxide layer, but the layer becomes highly nonuniform and nonadherent. Figure 1 shows the typical oscillogram for the programmed current experiment. We used 900 μs current pulse width and 10 ms between pulses (*v* = 100 Hz, 0.09 duty factor). The anodization voltage was monitored using a Tektronix oscilloscope.

The surface was examined using SEM micrographs for three samples of n-GaAs on which the oxide layer was grown under different conditions: constant voltage, constant current and pulsed constant current.

### 2.2. Cyclic voltammetry and chronopotentiometry studies

Cyclic voltammetry and chronopotentiometry experiments were also performed in the anodization solution. All experiments were carried out at room temperature (20 °C), in a classical three-electrode electrochemical cell using a PAR 173 potentiostat and a wave generator. The working electrode consisted of a 1 cm<sup>2</sup> n<sup>+</sup> GaAs, or 0.7 cm<sup>2</sup> n<sup>+</sup> GaAs substrate with p<sup>+</sup> 1 μm depth Zn diffusion wafers (the Zn diffusion was done using the ‘semiclosed box’ method at 650 °C). The counterelectrode was a platinum wire mesh and the reference electrode a saturated calomel electrode. The working electrode was prepared prior to each determination by applying a sufficiently cathodic potential (2 min at -3.5 V and -4.8 V for GaAs n<sup>+</sup> and p<sup>+</sup>, respectively) in the working solution for the native oxide layer to be completely removed.

\* Author to whom correspondence should be addressed.

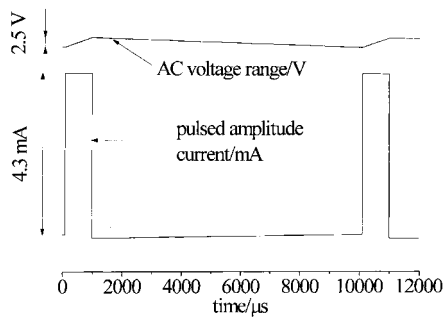


Fig. 1. Oscilloscope for the programmed current experiment used for pulsed constant current anodization of GaAs.

### 3. Results and discussions

#### 3.1. Pulsed constant current anodization of GaAs

Figure 1 shows the oscilloscope of current and voltage changes with time.  $900 \mu\text{s}$  wide current pulses are separated by 10 ms pauses between pulses. As a result, the measured d.c. voltage increases with time in a similar manner as for the continuous constant current case. Over this d.c. voltage a 2.5 V amplitude triangulated shape voltage variation is superposed, due to the pulsed anodic oxide growth. During the  $900 \mu\text{s}$  pulse width (current density on) the voltage was increased by 2–5 V which was necessary for oxide growth. After the current was dropped to zero, the layer stopped growing and the voltage was slowly decreased (between pulses).

The AGW electrolyte is a slight etchant [1] for GaAs oxides so that between pulses the layer is etched, possibly more in the nonuniform regions. Thus, a very uniform layer is obtained [3].

Assuming a  $1.926 \text{ nm V}^{-1}$  constant growth rate (obtained from the oxide thickness at 135 V final voltage) at  $4.3 \text{ mA cm}^{-2}$ , a 100 nm thick oxide layer is grown in only 12.5 min at  $j = 3.5 \text{ mA cm}^{-2}$  and 4.6 min at  $12 \text{ mA cm}^{-2}$ . If we relate this to the values from [2], of  $j = 120 \text{ mA cm}^{-2}$ , 100 nm grown in 5 min., it can be seen that the 100 nm anodization time is comparable at lower current densities.

Figure 2 presents typical plots of anodization voltage against time for constant current and for constant pulsed current conditions. The slopes corresponding to constant current conditions are about ten times greater, which agrees with the 1/10 duty factor for the pulsed current conditions. However, the values for pulsed current conditions are slightly lower than those corrected with the duty factor, probably because of the partial dissolution of the anodic film between pulses.

For defining emitter stripes in laser diodes, we need oxide layers thicker than 100 nm (for  $\text{SiO}_2$ ) and 150 nm (for anodic oxides). We obtained  $0.26 \mu\text{m}$  oxide thickness for  $j = 4.3 \text{ mA cm}^{-2}$  and 135 V final voltage. The whole anodization time was 18 min for this case (the 60 V final voltage process for  $17 \text{ mA cm}^{-2}$  takes only 1.66 min).

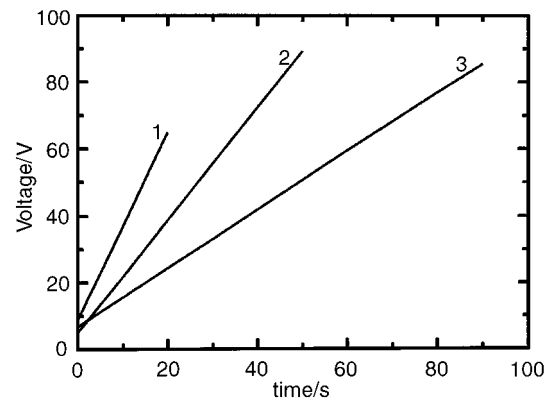


Fig. 2. Anodization voltage against time for constant current anodic growth. Current density,  $j/\text{mA cm}^{-2}$ : (1) 12, slope  $2.75 \text{ V s}^{-1}$ ; (2) 6, slope  $1.65 \text{ V s}^{-1}$  (3) 3, slope  $0.87 \text{ V s}^{-1}$ .

To obtain a high-quality beam in lateral dimensions for wide stripes, ridgewaveguide methods are used very frequently because of their simplicity. To control the difference between effective refractive indices inside and outside the stripe region, a very good control of the etch depth (10–20 nm) is needed. For this reason we need to elucidate what happens in the first moments of growth, when a voltage step is observed. This is why cyclic voltammetry and chronopotentiometry experiments were performed.

#### 3.2. Cyclic voltammetry studies

Cyclic voltammograms for both n and p-GaAs electrodes are shown in Figs 4 and 5, respectively. The shape of the voltammograms as well as the very large peak potential values suggest that the anodic oxidation of GaAs might verify the charge transfer with uncompensated cell resistance model developed by de Tacconi, Calandra and Arvia [8] based on the earlier paper of Gileadi and Srinivasan [9]. According to this model, the peak potential,  $V_{\text{max}}$ , is given by the following relationship:

$$V_{\text{max}} = a + b \times \ln v + c \times I_{\text{max}} \quad (1)$$

where  $a = RT/\beta F \ln [(\beta F/RT)(k/k_1)]$ ,  $b = (RT/\beta F)$  and  $c = R_u$

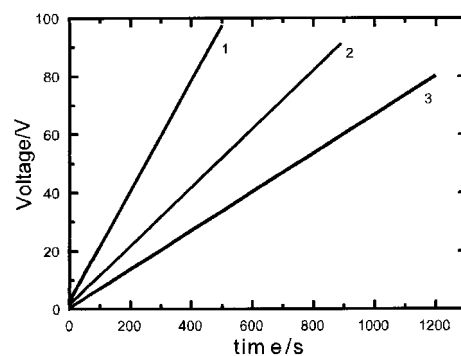


Fig. 3. Anodization voltage against time for pulsed constant current anodic growth. Current density,  $j/\text{mA cm}^{-2}$ : (1) 12, slope  $0.19 \text{ V s}^{-1}$ ; (2) 6, slope  $0.11 \text{ V s}^{-1}$ ; (3) 3, slope  $0.07 \text{ V s}^{-1}$ .

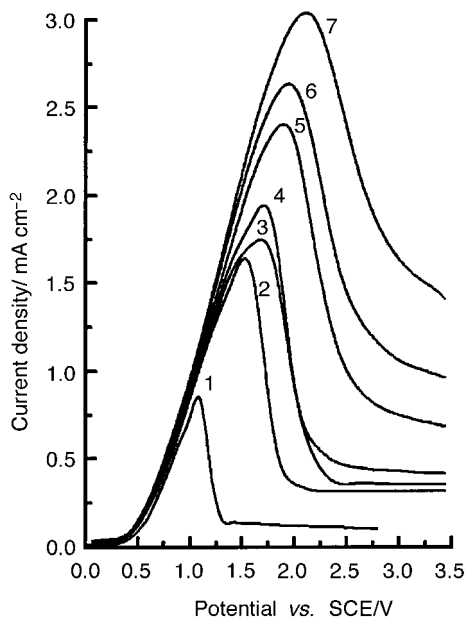


Fig. 4. Cyclic voltammograms for n-GaAs in AGW solutions. Scan rate,  $v/\text{mV s}^{-1}$ : (1) 3.45, (2) 34.5, (3) 46.0, (4) 69.0, (5) 172, (6) 230 and (7) 345.

In the above relationship,  $R_u$  ( $\Omega$ ) is the uncompensated cell resistance,  $k$  ( $\text{C m}^{-2}$ ) is the charge required to cover the electrode area with a monolayer of adsorbed intermediates  $k_1$  ( $\text{A m}^{-2}$ ) is the product between the rate constant of the forward reaction,  $k_1$ , and the anion activity in the bulk,  $a_{x^-}$ ,  $I_{\text{max}}$  is the current peak, and  $v$ , the scan rate [8]. After manipulations, using the least squares method, the values for  $a$ ,  $b$  and  $c$  coefficients, presented in Table 1 for both n and p-GaAs were found.

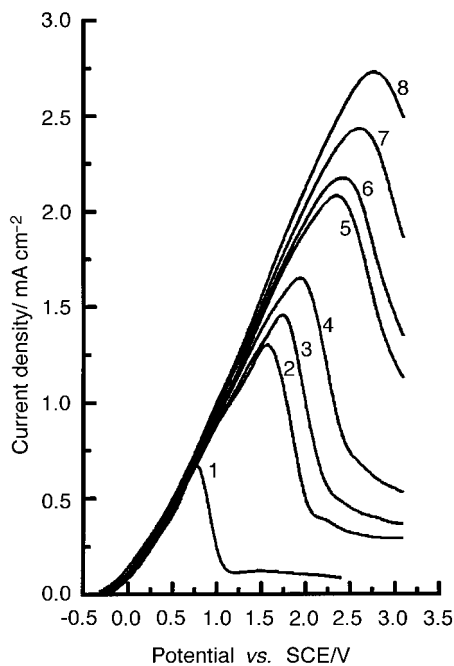


Fig. 5. Cyclic voltammograms for p-GaAs in AGW solutions. Scan rates,  $v/\text{mV s}^{-1}$ : (1) 3.45, (2) 34.5, (3) 46.0, (4) 69.0, (5) 138, (6) 172, (7) 230 and (8) 345.

Table 1. Coefficients  $a$ ,  $b$ , and  $c$  from Equation 1 for n and p-GaAs

Coefficient	n-GaAs	p-GaAs
$a/\text{V}$	1.24	1.75
$b/\text{V}$	0.051	0.208
$c/\Omega$	309	683

Table 2. Experimental and calculated data for cyclic voltametry of n- and p-GaAs in AGW mixture

$v/\text{V s}^{-1}$	n-GaAs			p-GaAs		
	$I_{\text{max}}/\text{mA}$	$V_{\text{max}}/\text{V}$ exp.	$V_{\text{max}}/\text{V}$ calc.	$I_{\text{max}}/\text{mA}$	$V_{\text{max}}/\text{V}$ exp.	$V_{\text{max}}/\text{V}$ calc.
0.00342	0.835	1.21	1.21	0.50	0.92	0.91
0.0342	1.58	1.54	1.55	0.90	1.62	1.66
0.0456	1.72	1.62	1.61	1.00	1.80	1.79
0.0684	1.90	1.70	1.69	1.12	1.96	1.96
0.1368	—	—	—	1.45	2.38	2.33
0.171	2.40	1.90	1.89	1.52	2.42	2.42
0.228	2.61	1.96	1.97	1.70	2.61	2.60
0.342	3.02	2.12	2.12	1.90	2.79	2.82

The experimental and calculated values for  $V_{\text{max}}$  are shown in Table 2 (the differences between the two values of  $R_u$  are due to the different geometry of the electrochemical cells used in the experiment). The  $RT/\beta F$  value for n-GaAs is very close to that for  $\beta = 0.5$  (0.0505 at 293 K); the corresponding value for p-GaAs is about four times greater but is in agreement with other values for anodic processes on p-GaAs [10].

### 3.3. Chronopotentiometry studies

For a better understanding of the initial anodization stages we performed several chronopotentiometric studies. The experimental results are shown in Fig. 6 and 7, for n-GaAs and p-GaAs, respectively. The chronopotentiometric results are consistent with those obtained by Szpak [12] who proposed a model for constant current anodic oxide growth, but without taking into account the uncompensated ohmic drop. However, it can be seen from the above data

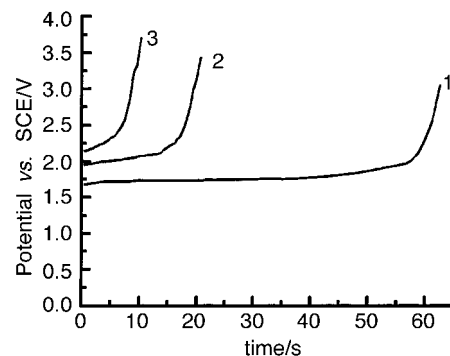


Fig. 6. Typical chronopotentiograms for constant current anodization of n-GaAs in AGW solution. Current density,  $j/\text{mA cm}^{-2}$ : (1) 1.0, (2) 1.5 and (3) 2.0.

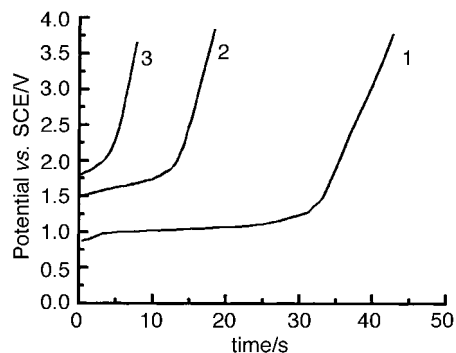


Fig. 7. Typical chronopotentiograms for constant current anodization of p-GaAs in AGW solution. Current density,  $j/\text{mA cm}^{-2}$ : (1) 1.0, (2) 1.5 and (3) 2.0.

that the ohmic drop is significant in this water–organic solvent mixture. The initial voltage step is mainly due to the electrolyte resistance for p-GaAs (Table 3). The corresponding values for n-GaAs are greater, because of potential drop on the reversely biased  $n^{2+}$  substrate needed for hole generation due to electrical breakdown in the high field region of the semiconductor beneath the contact. The depletion region for these highly doped wafers is  $\sim 0.025 \mu\text{m}$  before electrical breakdown [11]. For these highly doped wafers, illumination is not necessary for the anodic oxidation to take place.

If the charge transfer with uncompensated cell resistance model holds for these high current values, then the  $j\tau$  value (where  $\tau$  is the transition time in the chronopotentiogram, and  $j$  the imposed constant current density) must be constant, if we consider that the anodic layer starts growing only after the degree of electrode coverage is 1 [8]. However, this is not true, as can be seen from Table 3. This may be due to the fact that the anodic oxide growth starts earlier, before the electrode is fully covered; the current densities used for practical cases are much larger than those corresponding to the cyclic voltammograms at the lowest scan rate (which can be considered as steady-state polarization curves). Szpak [12] presumed the existence of a critical current density value (only above this critical value the anodic oxide layer starts growing).

### 3.4. SEM micrographs

Figure 8(a)–(c) show three SEM micrographs for n-GaAs anodic oxide grown in three different ways:

Table 3. Chronopotentiometry characteristics for n- and p-GaAs in AGW mixture

$j/\text{mAcm}^{-2}$	n-GaAs		p-GaAs	
	$\tau/\text{s}$	$V_{\text{initial step}}/\text{V}$	$\tau/\text{s}$	$V_{\text{initial step}}/\text{V}$
1.0	62.5	1.64	31.8	1.0
1.5	17.6	1.96	13.0	1.51
2.0	9.2	2.20	4.9	1.88

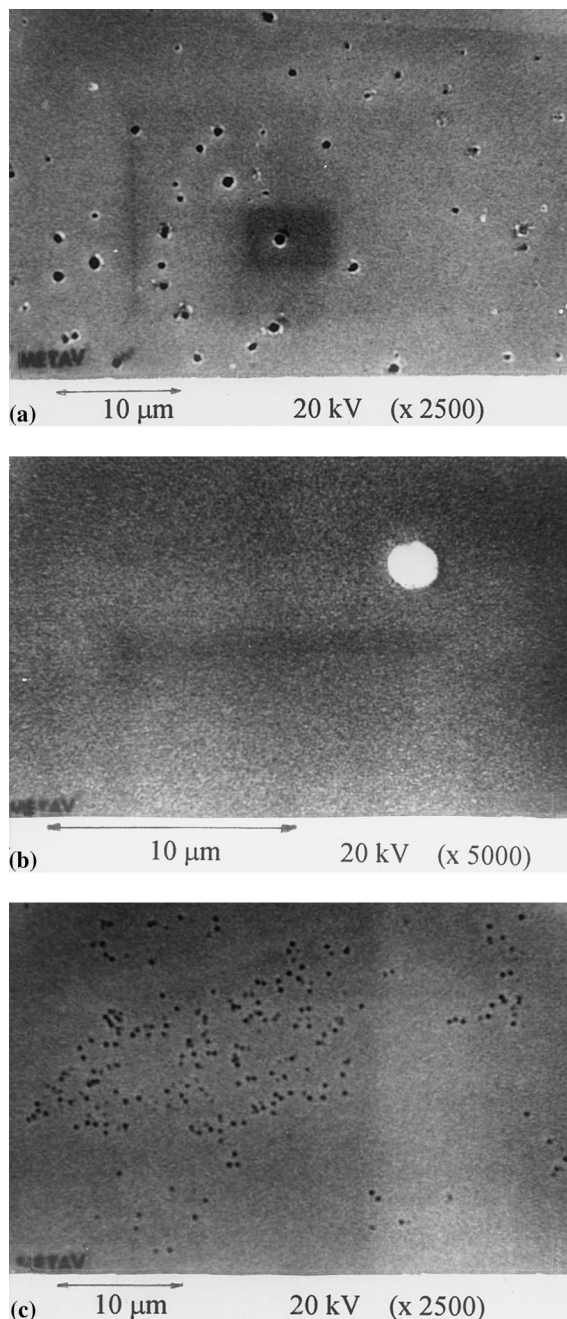


Fig. 8. SEM micrographs for three samples of n-GaAs anodized at a final voltage of 75 V in different conditions: (a) constant voltage, (b) pulsed constant current, and (c) constant current.

constant voltage, pulsed constant current and constant current conditions, respectively. The samples were anodized at a final voltage of 75 V.

The anodic oxide grown under constant voltage conditions shows relatively large holes with lifted edges, which might prove nonadherent in these zones. These holes are circular shaped,  $\sim 1 \mu\text{m}$  diameter. The anodic oxide grown in constant current conditions shows the same appearance, but the holes are much smaller ( $\sim 0.4 \mu\text{m}$ ) and the edges are flat. This appearance is in agreement with data presented by Szpak [12] for different anodization times in constant current conditions. The sample grown in pulsed constant current conditions is extremely uniform,

with no observable irregularities at  $\times 10\,000$  magnification.

#### 4. Conclusions

A  $0.26\ \mu\text{m}$  thick anodic oxide film at a final voltage of 135 V in anodic pulsed constant current conditions was obtained on  $\text{n}^{2+}$  GaAs wafers. A comparison was made between constant current and pulsed constant current conditions for anodic oxides on  $\text{n}^{2+}$  GaAs substrate. A 100 nm thick oxide layer is grown in only 12.5 min at  $j = 3.5\ \text{mA cm}^{-2}$  and 4.6 min at  $12\ \text{mA cm}^{-2}$ . The initial stages of anodic oxide growth were studied by means of cyclic voltammetry and chronopotentiometry, and can be described using the charge transfer with uncompensated cell resistance model [8]. The initial voltage step at anodic growth in constant current conditions, for this case, is mainly due to the electrolyte resistance for p-GaAs, whereas for n-GaAs the voltage drop for hole generation is added. The oxide surface was examined using SEM micrographs and the results show that the pulsed

constant current conditions offer the best anodic oxide growing in AGW mixtures.

#### References

- [1] H. Hasegawa and H. L. Hartnagel, *J. Electrochem. Soc.*, **123** (1976) 713.
- [2] M. J. Grove, D. A. Hudson and P. S. Zory, R. J. Dalby, C. M. Harding and A. Rosenberg, *J. Appl. Phys.*, **76** (1994) 587.
- [3] C. C. Largent, M. J. Grove, P. S. Zory, H. K. Choi and G. W. Turner, Proceedings of the SPIE Conference on 'Lasers and Applications', Photonics West '95, SPIE vol. 2382, pp. 244-49.
- [4] C. W. Fischer and S. W. Teare, *J. Appl. Phys.*, **67** (5), (1990) 2608.
- [5] A. J. Calandra, N. R. de Tacconi, R. Pereiro and A. J. Arvia, *Electrochim. Acta* **19** (1974) 901.
- [6] A. Yamamoto and S. Yano, *J. Electrochem. Soc.* **122** (1975) 260.
- [7] J. P. S. Pringle, *Electrochim. Acta* **25** (1980) 1423.
- [8] N. R. de Tacconi, A. J. Calandra and A. J. Arvia, *ibid.* **18** (1973) 571.
- [9] S. Srinivasan and E. Gileadi, *ibid.* **11** (1966) 321.
- [10] D. Meissner and R. Memming, *ibid.* **37** (1992) 799.
- [11] P. Blood, *Semicond. Sci. Technol.* **1** (1986) 7.
- [12] S. Szpak, *J. Electrochem. Soc.* **124** (1977) 107.